Available online at www.sciencedirect.com
SCIENCE DIRECT®
Catalysis Today 93–95 (2004) 735–742
CATALYSIS TODAY
www.elsevier.com/locate/cattod

Characterization of metal-containing molecular sieves and their catalytic properties in the selective oxidation of cyclohexane

Peng Tian, Zhongmin Liu*, Zongbin Wu, Lei Xu, Yanli He

Natural Gas Utilization and Applied Catalysis Laboratory, Dalian Institute of Chemical Physics, Chinese Academy of Sciences, P.O. Box 110, Dalian 116023, PR China

Available online 15 July 2004

Abstract

Three types of metal-containing molecular sieves with AFI, AEL and CHA structures (Me = Co, Mn, Cr and V) were synthesized hydrothermally and characterized by XRD, XRF, TG, TPR, NH_3-TPD and FT-IR. It was revealed that metals were incorporated into the framework of molecular sieves and induced the presence of charge centers. Both cobalt and manganese in the framework of AlPO-5, AlPO-11 and SAPO-34 were not reducible before the structure collapse. The redox behaviours of these catalysts in cyclohexane oxidation at 403 K using O_2 as oxidant were examined. CoAPO-11 exhibited best activity and good selectivities for the monofunctional oxidation products (88.5%). Cyclohexanol was the major product over most catalysts, whereas for Cr-containing molecular sieves, high selectivity of cyclohexanone was observed. Investigation of reaction mechanism based on CoAPO-11 and CrAPO-5 catalysts indicated that the decomposition of cyclohexyl hydroperoxide (CHHP), the intermediate in cyclohexane oxidation, followed the pathway: cyclohexanone ← CHHP → cyclohexanol → cyclohexanone.
© 2004 Elsevier B.V. All rights reserved.

Keywords: Metal-containing molecular sieve; Microporous aluminophosphate; Characterization; Cyclohexane; Oxidation

1. Introduction

Catalytic partial oxidations of hydrocarbons using oxygen or air as oxidant are significant and economical to the chemical industry [1,2]. Among various alkanes oxidation, the selective oxidation of cyclohexane is much attractive because its products are the intermediates for the manufacture of Nylon-6 and Nylon-6-6 [3]. Homogeneous catalysis using soluble transition metal salts (such as cobalt naphthenate) is the only technology, which had actually been developed until now. Since the cyclohexanol and cyclohexanone products are substantially more reactive than the cyclohexane reactant, high selectivities (>80%) to the sum of cyclohexanol and cyclohexanone only could be observed at low cyclohexane conversion (<5%). Moreover, it is very difficult to separate the catalysts from reaction mixture in the homogeneous system. Therefore, the development of effective recyclable solid catalysts could offer advantages.

Metal-containing molecular sieves have attracted great interests as catalysts since their appearance due to their acidity, redox, shape-selectivity and recyclable properties [4,5]. Up to now, many porous metal-containing molecular sieves with various structures have been synthesized and used as catalysts such as MeAPO, MeS-1 and MeMCM-41 (Me = Co, Mn, V, Cr, Fe, Ti, etc.) [6]. Information about the transition metal ions in molecular sieves would be beneficial to the understanding of their catalytic behaviours. A variety of works have been done to characterize the metal-containing molecular sieves, but the conclusions are still controversial. For example, the presence of Co^{3+} in the calcined state and the formation of bridged Co^{2+}-OH-P hydroxyl groups after reduction in CoAPO-18 were suggested by Chen et al. [7]; From the studies of UV–vis–NIR spectra, Sponer et al. [8] concluded that cobalt was present as Co^{2+} in cobalt-containing aluminophosphate molecular sieves and did not change its valence during calcination.

Liu and Weng [9] first reported the use of CoAPO-5 as heterogeneous catalysts for cyclohexane oxidation in acetic acid as solvent. Unfortunately, further investigations [10] revealed that unavoidable leaching of cobalt from the framework with the use of acetic acid contributed to the observed

* Corresponding author. Tel.: +86 411 84685510; fax: +86 411 84691570.
E-mail addresses: liuzm@dicp.ac.cn, zml@dicp.ac.cn (Z. Liu).

0920-5861/$ – see front matter © 2004 Elsevier B.V. All rights reserved.
doi:10.1016/j.cattod.2004.06.100

results. Thomas and co-workers [11,12] published interesting works using MeAPOs as effective catalysts for the selective cyclohexane oxidation. They found that the structure of molecular sieves influenced the metal valence in the calcined samples and caused different alkane oxidation activity.

In this paper, we prepared pure and highly crystalline MeAPO-5, MeAPO-11 and MeAPSO-34 molecular sieves (Me = Co, Mn, Cr and V). Many methods such as TG, TPR, TPD of NH_3 and FT-IR were used to investigate the nature of metals in those samples. Their catalytic behaviours in cyclohexane oxidation without the use of a solvent were studied in detail using molecular oxygen as oxidant.

2. Experimental

2.1. Synthesis

MeAPO-5, MeAPO-11 and MeAPSO-34 were synthesized hydrothermally according to the literatures [13,14]. The aluminium, phosphorus and silicon sources were pseudoboehmite, H_3PO_4 (85%) and silica sol (25 wt.%), respectively. Cobalt (II) acetate, manganese (II) acetate, chromium (III) nitride, vanadyl acetate, iron (II) sulphate and titanium (IV) sulphate were used as metal sources. The templating agents were triethylamine for MeAPO-5 and MeAPSO-34 and *n*-dipropylamine for MeAPO-11. The synthesis conditions were given in Table 1. As-synthesized molecular sieves were calcined in air at 823 K for 5 h to remove organic template.

2.2. Characterization

XRD measurement was carried out using Rigaku X-ray diffractometer (Model D/Max-γB) with Cu Kα radiation.

The metal content in the molecular sieves was measured by XRF (Philips Magix).

TG analysis was recorded on Perkin Elmer Pyriss TGA with a heating rate of 5 K/min from 323 to 973 K under air (35 ml/min).

TPD of NH_3 and TPR experiments were carried out with Autowin 2910 equipment (Micromeritics). All the samples (40–60 mesh) were first activated at 873 K (10 K/min) for 30 min under 20 ml/min of He (for TPD) or Ar (for TPR). For NH_3-TPD, ammonia was injected to saturate the sample at 383 K. The measurement of desorbed NH_3 was performed from 383 to 823 K (10 K/min) under He (40 ml/min). For TPR, H_2/Ar mixture (H_2/Ar molar ratio of 0.1 and a total flow of 40 ml/min) was used and the reactor was heated from room temperature to 1023 K (10 K/min).

FT-IR spectra of pyridine adsorption were recorded on a Bruker EQUINOX55 with a resolution of 2 cm^{-1}. Self-supporting wafers of about 5 mg/cm^2 were first activated in situ in an IR cell at 773 K in high vacuum for 4 h. Pyridine was admitted into the cell at room temperature and after 10 min equilibrium, pyridine was desorbed at 298, 423 and 573 K under high vacuum during 1 h. All the spectra were recorded at room temperature.

2.3. Catalytic reaction

Cyclohexane oxidation was carried out in a 100 ml autoclave lined with polytetrafluoroethylene (PTFE). Typically, 18 g cyclohexane, about 0.7 g catalyst (0.195 mmol metal) and 0.04 g tetrabutyl hydroperoxide (TBHP, used as initiator) were introduced into the reactor. After charged 1.1 MPa of O_2, the reactor was heated to 403 K under stirring within half an hour and hold at this temperature for 3 h. When the reaction was finished, 20 ml ethyl alcohol was added into the cold reactor to dissolve carboxylic acids. The catalyst

Table 1
Gel compositions and metal content in the molecular sieves

Sample	Gel compositions						Crystallization		Me (wt.%)
	R	Al_2O_3	P_2O_5	SiO_2	MeO	H_2O	Time (h)	*T* (K)	
AlPO-5	1.2	1	1	0	0	50	40	448	–
CoAPO-5	1.2	1	1	0	0.05	50	40	448	1.62
MnAPO-5	1.2	1	1	0	0.05	50	40	448	1.76
CrAPO-5	1.2	1	1	0	0.05	50	40	448	0.95
VAPO-5(1)	1.2	1	1	0	0.05	50	40	448	0.37
VAPO-5(2)	1.2	1	1	0	0.25	50	40	448	1.07
FeAPO-5	1.2	1	1	0	0.05	50	40	448	1.82
TiAPO-5	1.2	1	1	0	0.05	50	40	448	0.49
AlPO-11	1.0	1	1	0	0	50	40	473	–
CoAPO-11	1.0	1	1	0	0.05	50	40	473	1.14
MnAPO-11	1.0	1	1	0	0.05	50	40	473	1.25
CrAPO-11	1.0	1	1	0	0.05	50	40	473	1.08
VAPO-11	1.0	1	1	0	0.05	50	40	473	0.66
CoAPSO-5	1.2	1	1	0.2	0.05	50	40	448	1.58
CoAPSO-11	1.1	1	1	0.2	0.05	50	72	473	1.62
CoAPSO-34	3	1	1	0.2	0.08	50	48	473	2.2
MnAPSO-34	3	1	1	0.2	0.05	50	48	473	1.32

was separated by centrifugation. The reaction products were analyzed on a Varian CP-3800 gas chromatograph equipped with an FFAP capillary column (0.53 mm × 25 m) and an FID detector. The conversion was calculated based on the starting cyclohexane. As cyclohexyl hydroperoxide (CHHP) partially decomposed upon injection, its concentration was estimated by double analysis, before and after reducing CHHP to cyclohexanol with Ph_3P [15].

3. Results and discussion

3.1. XRD studies

The typical XRD patterns of as-synthesized molecular sieves are shown in Fig. 1. MeAPO-5 with AFI topology belongs to the 12-member ring group with one-dimensional circular channel system. It has large pore opening of 0.73 nm. MeAPO-11 with AEL structure and elliptical channel (0.65 nm × 0.4 nm) is a medium pore molecular sieve. MeAPSO-34 with three-dimensional channel has smaller pore (0.38 nm) and a structure similar to the one of natural chabazite (CHA).

The XRD patterns illustrate the rather high crystallinity of all samples. No extra peak related to transition metal oxides appeared, indicating the purity of the products.

The synthesis conditions and metal amounts in the molecular sieves are displayed in Table 1. Most molecular sieves had metal contents in the products close to those in starting gels despite some variation. But for VAPO-5, TiAlPO-5 and VAPO-11, the metal contents in the products were unexpectedly low. The low Ti content may be due to the use of inorganic titanium precursor in the starting gel. The V content in VAPO-5 could be enhanced from 0.37 to 1.17 wt.% by increasing the V/P molar ratio in the synthesis gel from 0.025 to 0.125 (see Table 1), in agreement with the work of Blasco et al. [16].

3.2. Thermal analysis

Fig. 2 illustrates the thermogravimetric (TG) curves of MeAPO-5 and MeAPO-11. The TG curves of AlPO-5 and AlPO-11 are shown in Fig. 2 for comparison. Three-step weight losses could be observed in the 323–373, 373–523 and 523–893 K temperature ranges for MeAPO-5 and in the 323–373, 373–543 and 543–893 K temperature ranges for MeAPO-11. The initial step corresponded to water desorption and the second one to template desorption. The third step weight loss was ascribed to the combustion of some organic species occluded in the channels of MeAPOs. The results of weight losses for each step are collected in Table 2.

It can be seen that the water content (∼3.2 wt.%) and organic template content (∼8.5 wt.%) in all MeAPO-5s and AlPO-5 samples remained nearly the same. The template amount corresponded to ∼1.3 molecules of TEA per unit cell. However, careful examination revealed that the ratio of the template removal in the second step to that in the third step was very different between AlPO-5 and MeAPO-5s. About 3/4 of the total template was removed during the second step in AlPO-5, whereas only 1/2 in this step for all MeAPO-5s. As the charge of AlPO-5 framework is neutral and the organic template is filled physically in the pores, it is expected that most of the template could be eliminated at lower temperatures. The increased weight loss of metal-containing AlPO-5s at higher temperatures clearly indicated that there existed strong interactions between the framework of MeAPO-5s and the template, which made TEA molecules strongly bonded in MeAPO-5s. Other authors [16–18] have also observed the similar experimental results for metal-containing aluminophosphate molecular

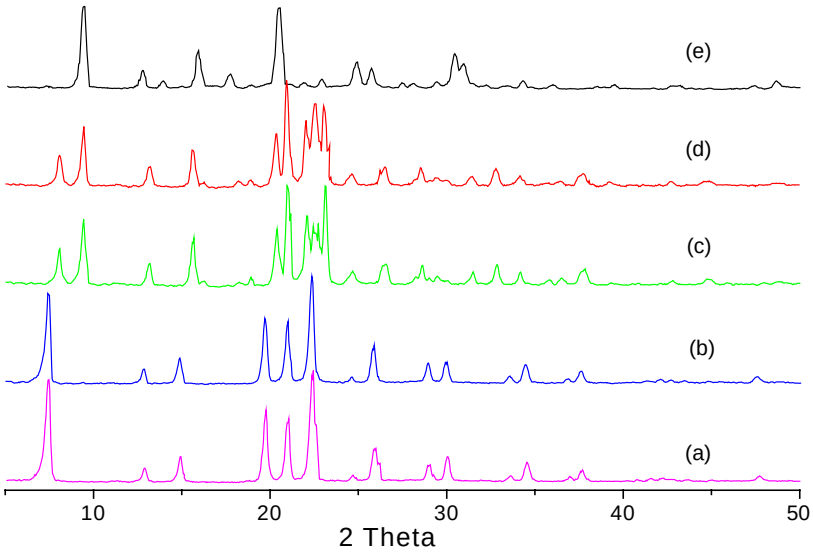

Fig. 1. XRD patterns of (a) CoAPO-5, (b) MnAPO-5, (c) CoAPO-11, (d) MnAPO-11 and (e) CoAPSO-34.

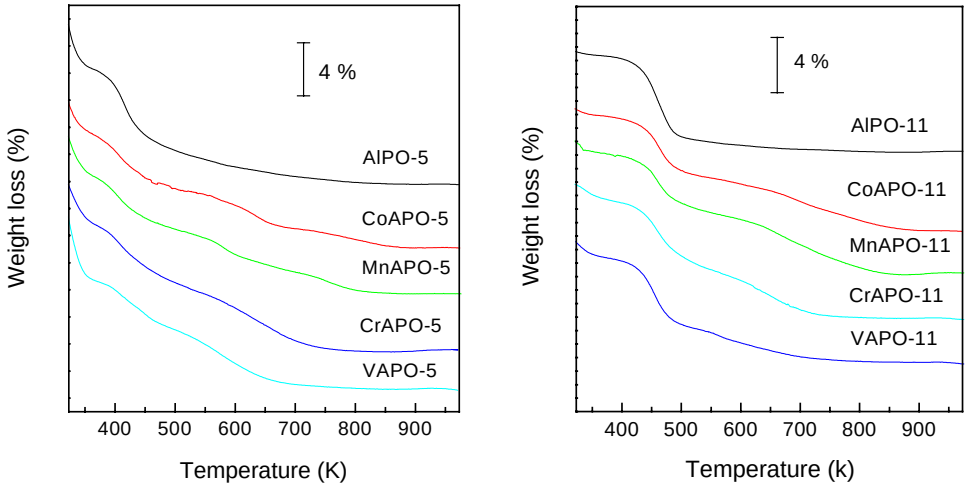

Fig. 2. TG curves of as-synthesized metal-containing aluminophosphate molecular sieves.

Table 2
TG results of MeAPO-5, 11

Sample	Weight loss (wt.%)			Template weight loss (wt.%)	Total weight loss (wt.%)
	1-Step	2-Step	3-Step		
AlPO-5	3.3	6.2	2.1	8.3	11.6
CoAPO-5	3.2	4	4.2	8.2	11.2
MnAPO-5	3.0	3.9	4.6	8.5	11.5
CrAPO-5	3.1	4.5	4.6	9.1	12.2
VAPO-5(2)	3.7	3.6	4.3	7.9	11.6
AlPO-11	0.3	6.5	0.7	7.2	7.4
CoAPO-11	0.5	4.7	3.9	8.6	9.1
MnAPO-11	0.6	4.6	4.3	8.9	9.5
CrAPO-11	1.2	5.3	3.3	8.6	9.8
VAPO-11	1.2	5.2	2.5	7.7	8.9

sieves (Me = Co, Mn, V, etc.). This is usually taken as a proof that charge deficiency had been induced in the framework by isomorphous substitution of transition metals.

For AlPO-11 and MeAPO-11s, more template molecules were occluded in MeAPO-11s than in AlPO-11 from TG results (see Table 2). However, the difference of template removal in the second and third steps between AlPO-11 and MeAPO-11s was similar to that between AlPO-5 and MeAPO-5s. It can be inferred that transition metals (Me = Co, Mn, V, Cr), at least large amount of them, incorporated into the framework during hydrothermal synthesis and induced the appearance of the charge deficiency.

3.3. Temperature-programmed reduction

The TPR profiles of Co- and Mn-containing samples are given in Fig. 3. The two peaks centred at 633 and 833 K on Co/AlPO-11 (1.6 wt.% Co) were due to the reduction of Co_3O_4 and CoO (or Co species interacting strongly with support), respectively [19–21]. For CoAPO-5, CoAPO-11 and CoAPSO-34, no peak was detected at lower temperature and H_2 consumption only occurred after 973 K, which could be caused by the reduction of non-framework cobalt and aluminium species, formed after the collapse of molecular sieves structures [22]. The difference of TPR curves

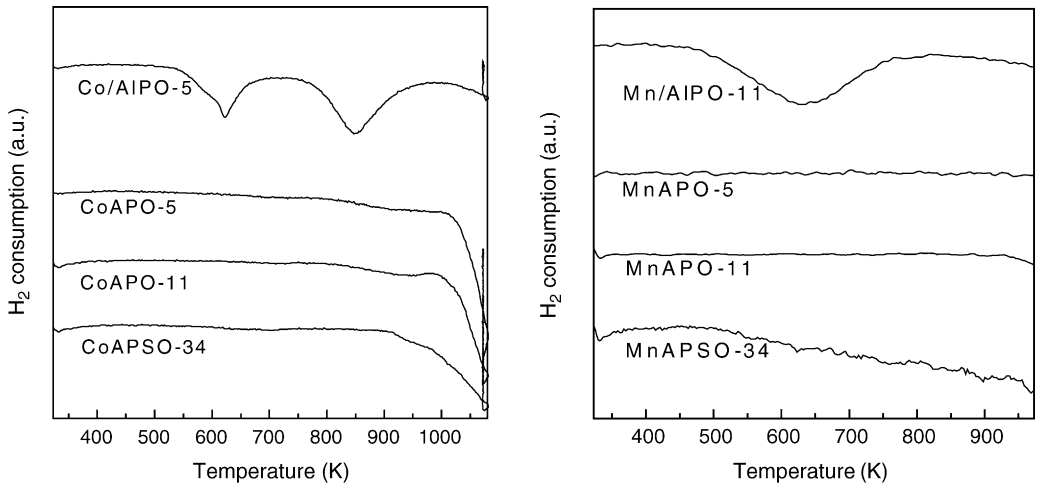

Fig. 3. TPR results of MeAPO-5, 11, MeAPSO-34 and Me/AlPO-11.

between supported and synthesized Co-containing samples demonstrates that cobalt species existed in the framework of all Co-containing molecular sieves and were not reducible, in agreement with the above TG results and the work of Berndt, who studied TPR of CoAPO-5 and CoAPO-44 and obtained the similar results [21].

The supported sample Mn/AlPO-11 (1.6 wt.% Mn) presented one reduction peak with maximum at 633 K, whereas no H_2 consumption appeared on MnAPO-5, 11 and MnAPSO-34 before 973 K. This indicates that manganese species existed in the framework and were not easily reduced, with the same behaviour as CoAPO-5, 11 and CoAPSO-34.

3.4. TPD of ammonia

NH_3-TPD was used in order to characterize the acidity of Co, Mn-containing AlPOs. The results are shown in Fig. 4. The comparison of the TPD curves of MeAPOs with that of AlPO-5 indicated a increase of the acid strength and amount. The peak with maximum at about 473 K, found for all samples, was due to weakly bonded ammonia (physisorbed ammonia, ammonia adsorbed on weak Lewis sites and terminal P-OH groups) [23]. The high temperature peak centred at around 653 K, which was not detectable on AlPO-5, could be ascribed to ammonia desorbed from strong acid sites in MeAPOs. The presence of the high temperature of ammonia desorption suggests that charge centres (Brønsted and/or Lewis acid sites) existed in the calcined Co, Mn-containing AlPO-5, 11. The strength of acid sites decreased in the following order: CoAPO-11 > MnAPO-11 ≈ CoAPO-5 > MnAPO-5 > AlPO-5.

3.5. FT-IR spectra of pyridine adsorption

The FT-IR spectra of pyridine adsorbed on Co-, Mn-containing molecular sieves after desorption at 423 and 573 K are presented in Fig. 5. Generally, in the case of pyridine sorption, bands at 1548 and 1450 cm^{-1} are indicative of Brønsted and Lewis acid sites, respectively. The band at 1490 cm^{-1} is associated with both Brønsted and Lewis acid sites. The ratio of Brønsted/Lewis (displayed in Table 3) can be estimated using the relative surfaces of the Brønsted and Lewis bands and the molar absorption coefficients of these two sites calculated by Guisnet et al. [24] ($\varepsilon_B = 1.13$, $\varepsilon_L = 1.28$ cm μmol^{-1}).

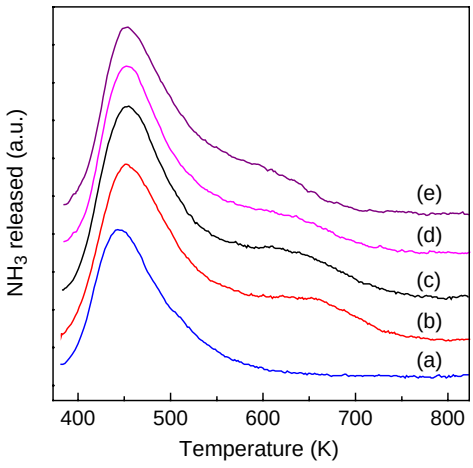

Fig. 4. NH_3-TPD of (a) AlPO-5, (b) CoAPO-11, (c) CoAPO-5, (d) MnAPO-11 and (e) MnAPO-5.

Table 3
B/L acid sites on Co and Mn containing AlPO-5 and AlPO-11 molecular sieves

Sample	Brønsted/Lewis[a]	
	423 K	573 K
CoAPO-5	0.27	0.43
MnAPO-5	0.26	0.36
CoAPO-11	0.36	0.48
MnAPO-11	0.24	0.44

[a] $\varepsilon_L/\varepsilon_B$ • 1.13, using extinction coefficients by Guisnet et al. [24].

All samples exhibited bands at 1548 and 1450 cm^{-1}, even after desorption at 573 K, suggesting that there existed strong acid sites (both Brønsted and Lewis acid) in Co-, Mn-containing AlPO-5 and AlPO-11. After desorption at 423 K, all four samples presented a large proportion of Lewis acid sites. The distribution of acid sites at 573 K was not significantly modified, except for a slight decrease of the peak intensities. It confirms, as already noticed in NH_3-TPD studies, that charge centres (Brønsted and Lewis acid sites) existed in the calcined Co-, Mn-containing AlPO-5 and AlPO-11.

3.6. Cyclohexane oxidation

The catalytic activity of metal-containing AlPO-5, 11 and SAPO-34 had been studied in cyclohexane oxidation using molecular oxygen as oxidant. Table 4 presents the oxidation results. All Co-, Mn-, Cr- and V-containing molecular sieves showed catalytic oxidation activity, whereas TiAPO-5 and FeAPO-5 gave as low reactivity as AlPO-5 catalyst. CoAPO-11 and MnAPO-11 exhibited best activity and all MeAPO-11 catalysts showed better activity than corresponding MeAPO-5s and MeAPSO-34s. Compared with MeAPO-5 and -11, MeAPSO-34 only possesses smaller pore openings so that cyclohexane molecule cannot access its inside. The transition metals on the external surface of MeAPSO-34 maybe contributed to the observed activities.

Good selectivity of monofunctional oxidation products (cyclohexanol, cyclohexanone and cyclohexyl hydroperoxide) was observed on CoAPO-11, although it had highest cyclohexane conversion of 7.8%. Cyclohexanol was the preferable product on most catalysts except for CrAPO-5 and -11. High selectivity of cyclohexanone was observed on Cr-containing catalysts, in agreement with the work of Chen and Sheldon [25]. They investigated the cyclohexane

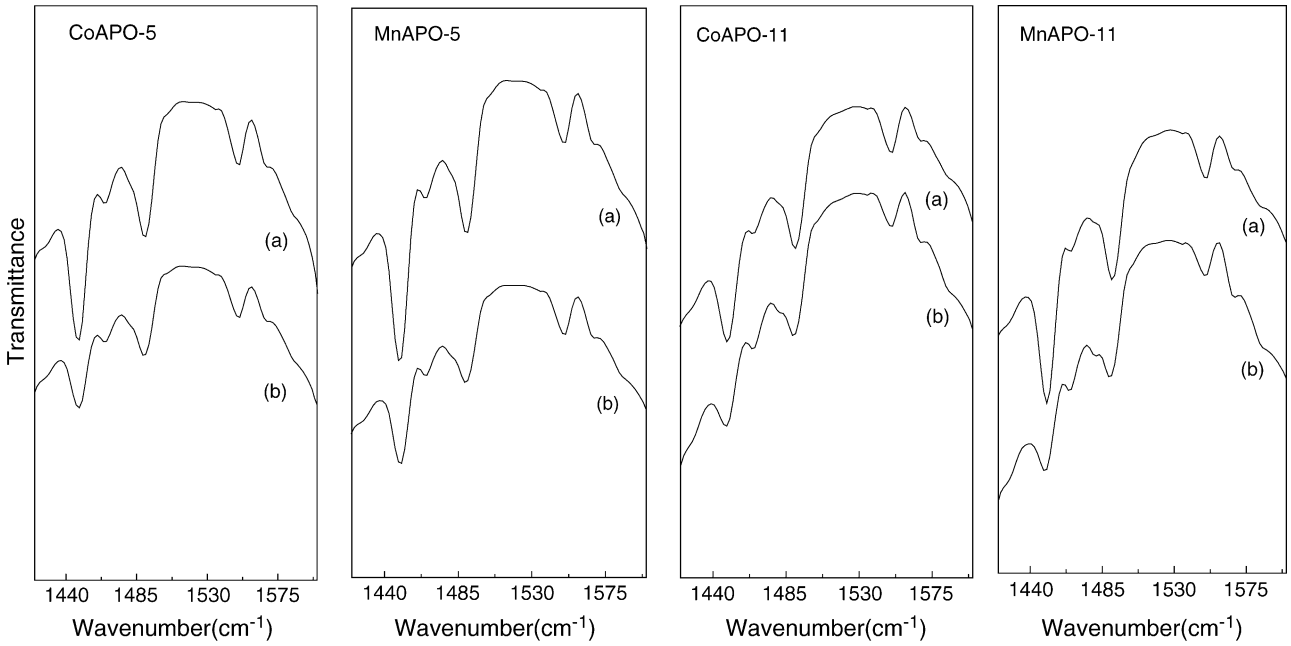

Fig. 5. FT-IR spectra of pyridine adsorption on MeAPO-5 and MeAPO-11 molecular sieves (a) desorption at 423 K and (b) desorption at 573 K.

oxidation on CrAPO-5 and found low ratios of cyclohexanol to cyclohexanone regardless of reaction temperature and time. Both VAPO-5 and -11 showed the ability of deep oxidation due to the low selectivity of monofunctional oxidation products. Therefore, both metal types and structure of molecular sieves had influence on reaction activity and selectivity.

Acidic CoAPSO-5 and CoAPSO-11 were also tested as catalysts and gave much lower conversion than corresponding CoAPO-5 and CoAPO-11 (see Table 4). This was possibly due to the increased interaction between the acid channels and the polar oxidation products, which caused the slow diffusion and the poor catalytic behaviour.

The kinetic studies were performed on CoAPO-5 (Fig. 6). Because small amount of TBHP was added into the reaction mixture, no induction time was observed. Cyclohexane conversion and selectivity of cyclohexanone increased with time during the reaction time of 3 h. The ratio of cyclohexanol/cyclohexanone, the selectivity of cyclohexanol, CHHP and the monofunctional oxidation products decreased following the reaction time.

It is reported that CHHP is the intermediate of the cyclohexane oxidation and its formation is the rate-determining step [26]. Two mechanisms exist for CHHP rapid decomposition: heterolytic (CHHP → cyclohexanone) and homolytic

Table 4
Cyclohexane oxidation on MeAPO-5, -11 and MeAPSO-34 at 403 K for 3 h[a]

Catalyst	Conversion (%)	TON ($mol_{substrate}\ h^{-1} mol_{metal}^{-1}$)	Product distribution (mol%)[b]				
			A	B	CHHP	Others	B/A
CoAPO-5	5.0	18.3	38.1	44.6	4.2	13.1	1.2
MnAPO-5	3.1	11.4	26.2	46.5	16.4	10.9	1.8
CrAPO-5	5.9	21.6	61.0	19.9	5.0	14.1	0.3
VAPO-5(2)	2.9	10.6	24.5	31.8	0	43.7	1.3
FeAPO-5	0.7	2.6	12.4	31.3	51.4	4.9	2.5
TiAPO-5	0.5	1.8	19.1	36.8	17.6	26.5	1.9
CoAPO-11	7.8	28.6	43.6	43.1	1.8	11.5	1.0
MnAPO-11	7.6	27.8	33.6	43.9	3.8	18.7	1.3
CrAPO-11	6.1	22.3	58.5	17.1	8.4	16.0	0.3
VAPO-11	4.3	15.8	42.0	35.5	0	22.5	0.8
CoAPSO-34	2.9	10.6	25.0	43.8	22.2	9.0	1.8
MnAPSO-34	2.8	10.3	24.4	45.2	23.7	6.7	1.9
CoAPSO-5	2.5	9.2	18.0	46.4	27.4	8.2	2.6
CoAPSO-11	2.7	9.9	17.0	39.2	34.6	9.2	2.3
AlPO-5	0.7	-	10.9	46.4	25.0	17.7	4.3

[a] Catalyst (0.195 mmol metal), 18 g cyclohexane, 0.04 g TBHP, 1.1 MPa O_2, 403 K, 3 h.
[b] A: cyclohexanone, B: cyclohexanol and CHHP: cyclohexyl hydroperoxide.

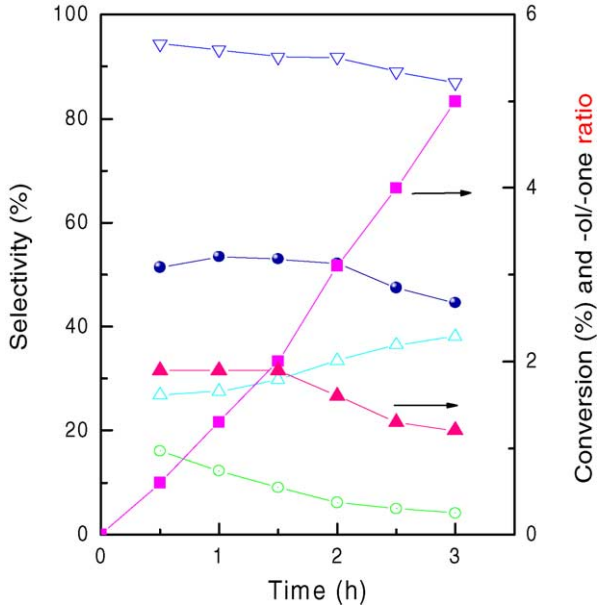

Fig. 6. Conversion and selectivity of cyclohexane oxidation on CoAPO-5. Conversion (■); ratio of cyclohexanol to cyclohexanone (▲); selectivity of cyclohexanol (●), cyclohexanone (△), CHHP (○), total selectivity of cyclohexanone, cyclohexanol and CHHP (▽).

Table 5
Comparison of cyclohexane and cyclohexanol oxidation in the presence of solvent

Catalyst	Solvent	Substrate	Conversion (%)	Yield (%)[a]	ol/one[b]
CoAPO-11[c]	CH_3CN	Cyclohexane	8.4	–	1.2
CoAPO-11[d]	CH_3CN	Cyclohexanol	10.9	10.5	–
CrAPO-5[c]	CH_3CN	Cyclohexane	7	–	0.2
CrAPO-5[d]	CH_3CN	Cyclohexanol	19.6	17.2	–

Reaction conditions: 403 K, 3 h, MeAPO (0.195 mmol metal), TBHP (0.03 g), O_2 1.1 MPa.
[a] Yield of cyclohexanone.
[b] Ratio of cyclohexanol/cyclohexanone.
[c] Cyclohexane (10 g) + solvent (10 g).
[d] Cyclohexanol (0.36 g) + solvent (18 g).

(CHHP → cyclohexanol). In addition, cyclohexanol is more active than cyclohexane under reaction conditions and can be converted to cyclohexanone easily. So there are two possible pathways for the products formation:

(1) CHHP → cyclohexanol → cyclohexanone
(2) cyclohexanone ← CHHP → cyclohexanol (then cyclohexanol → cyclohexanone)

In order to distinguish the above pathways, designed experiments were performed based on CoAPO-11 and CrAPO-5. The results are shown in Table 5. About 8.4 and 7% of cyclohexane conversion on CoAPO-11 and CrAPO-5 with acetonitrile as solvent were obtained. The corresponding cyclohexanol/cyclohexanone ratios were 1.2 and 0.2 for them, respectively. If the reaction process followed the pathway (1) during oxidation, cyclohexanol conversion at the similar reaction conditions should be of around 45 and 83% on CoAPO-11 and CrAPO-5, in order to reach cyclohexanol/cyclohexanone ratios of 1.2 and 0.2. However, Table 5 shows that cyclohexanol gave only 10.9 and 19.6% yield of cyclohexanone on CoAPO-11 and CrAPO-5. These values were much lower than expected. Therefore, pathway (2) should be more reliable, that is, both heterolytic and homolytic mechanisms existed during CHHP decomposition. The difference between the two catalysts was that homolytic mechanism of CHHP decomposition occupied a large proportion on CoAPO-11, whereas heterolytic mechanism occurred predominantly on CrAPO-5.

4. Conclusion

The present work demonstrated that TG, NH_3-TPD and TPR could be used as effective methods to characterize the metal-containing molecular sieves. The characterization results confirmed that metals existed into the molecular sieves framework and charge deficiency was created by the incorporation of metals. Co and Mn were not reducible before 973 K in the lattice position.

In cyclohexane oxidation, all MeAPO-11s had better activity than corresponding MeAPO-5s and MeAPSO-34s. CoAPO-11 exhibited the best activity and good selectivity of monofunctional oxidation products. Acidic molecular sieves had negative effect on the oxidation reaction. Both heterolytic and homolytic mechanisms existed in the decomposition of CHHP on CoAPO-11 and CrAPO-5.

References

[1] R.A. Sheldon, J.K. Kochi, Metal-catalyzed Oxidations of Organic Compounds, Academic Press, New York, 1981.
[2] K.A. Suresh, M.M. Sharma, T. Sridhar, Ind. Eng. Chem. Res. 39 (2000) 3958.
[3] U. Schuchardt, D. Cardoso, R. Sercheli, R. Pereira, R.S. Da Cruz, M.C. Guerreiro, D. Mandelli, E.V. Spinace, E.L. Pires, Appl. Catal. A 211 (2001) 1.
[4] R.A. Sheldon, I.W.C.E. Arends, H.E.B. Lempers, Catal. Today 41 (1998) 387.
[5] J.M. Thomas, R. Raja, Chem. Commun. (2001) 675.
[6] M. Hartmann, L. Kevan, Chem. Rev. 99 (1999) 635.
[7] J. Chen, J.M. Thomas, G. Sankar, J. Chem. Soc., Faraday Trans. 90 (1994) 3455.
[8] J. Sponer, J. Cejka, J. Dedecek, B. Wichterlova, Micropor. Mesopor. Mater. 37 (2000) 117.
[9] S.S. Lin, H.S. Weng, Appl. Catal. 105 (1993) 289.
[10] I. Belkhir, A. Germain, F. Fajula, E. Fache, J. Chem. Soc., Faraday Trans. 94 (1998) 1761.
[11] G. Sankar, R. Raja, J.M. Thomas, Catal. Today 55 (1998) 15.
[12] M. Dugal, G. Sankar, R. Raja, J.M. Thomas, Angew. Chem. Int. Edit. 39 (2000) 2310.
[13] S.T. Wilson, E.M. Flanigen, US Patent 4,567,029 (1986).
[14] J. Tan, Z.M. Liu, X.H. Bao, X.C. Liu, X.W. Han, C.Q. He, R.S. Zhai, Micropor. Mesopor. Mater. 53 (2002) 97.
[15] G.B. Shulpin, D. Attanasio, L. Suber, J. Catal. 142 (1993) 147.

[16] T. Blasco, P. Concepcion, J.M. Lopez Nieto, J. Perez-Pariente, J. Catal. 152 (1995) 1.
[17] Y.H. Yeom, S.C. Shim, J. Mol. Catal. A 180 (2002) 133.
[18] C. Montes, M.E. Davis, B. Murray, M. Narayama, J. Phys. Chem. 94 (1990) 6425.
[19] Y.L. Zhang, D.G. Wei, S. Hammache Jr., J.G. Goodwin, J. Catal. 188 (1999) 281.
[20] J. Panpranot Jr., J.G. Goodwin, A. Sayari, Catal. Today 77 (2002) 269.
[21] H. Berndt, A. Martin, Y. Zhang, Micropor. Mater. 6 (1996) 1.
[22] R. Roque-Malherbe, R. Lopez-Cordero, J.A. Gonzales-Morles, J. Onate-Martinez, M. Carreras-Gracial, Zeolites 13 (1993) 481.
[23] M. Hochtl, A. Jentys, H. Vinek, Micropor. Mesopor. Mater. 31 (1999) 271.
[24] M. Guisnet, P. Ayrault, C. Coutanceau, M.F. Alvarez, J. Datka, J. Chem. Soc., Faraday Trans. 93 (1997) 1661.
[25] J.D. Chen, R.A. Sheldon, J. Catal. 153 (1995) 1.
[26] R. Pohorecki, J. Baldyga, W. Moniak, W. Podgorska, A. Zdrojkowski, P.T. Wierzchowski, Chem. Eng. Sci. 56 (2001) 1285.